RESEARCH PAPER

Hydrothermal Synthesis of an Ethiodol Based Ferrofluid as a Potential MRI Contrast Agent

Reza Ahmadi[1,*], *Narges Shahbazi*[2]

[1] *Department of Materials Engineering, Imam Khomeini International University, Qazvin, Iran*

[2] *Department of Nonobiotechnology, Tarbiat Modares University, Tehran, Iran*

ARTICLE INFO

Article History:
Received 04 November 2018
Accepted 16 December 2018
Published 01 January 2019

Keywords:
Biocompatibility
Ethiodol
Hydrothermal
Magnetite
MRI

ABSTRACT

In the present work, stable ferrofluids containing oleic acid capped magnetite nanoparticles were synthesized via low temperature hydrothermal method. The physical and chemical properties of the synthesized particles were studied using TEM, XRD, AFM, VSM and PCS techniques. Mean particles size of the samples was between 4.5 and 10 nanometers, depending on experimental conditions. Effect of precursor's medium alkalinity was investigated on particle size. Cell culture experiments performed via MTT assay demonstrated that this product was biocompatible. In addition, cellular uptakes were investigated by Prussian blue staining and also measuring Fe concentration by inductively coupled plasma spectroscopy. Finally, the synthesized particles were dispersed in the Ethiodol and the obtained suspension was used as a potential MRI contrast agent. To the best of our knowledge, the mentioned procedure of using a non-aqueous based MRI contrast agent has been done for the first time in the present work and provides good capabilities as opposed to aqueous ones including reduced synthesis process time and increased magnetic properties of the obtained contrast agent.

How to cite this article
Ahmadi A, Shahbazi N. Hydrothermal Synthesis of an Ethiodol Based Ferrofluid as a Potential MRI Contrast Agent. J Nanostruct, 2019; 9(1): 14-20. DOI: 10.22052/JNS.2019.01.003

INTRODUCTION

Ceramic nanoparticles especially transition and rare earth metal oxides such as Fe_2O_3, Fe_3O_4, MnO, Mn_3O_4 and Gd_2O_3 nanoparticles have been recently synthesized and used as potential negative and positive MRI contrast agents [1-5]. These applications are mainly due to the large number of unpaired electrons and short electron spin relaxation times of iron, manganese and gadolinium ions. Thus, they strongly affect the proton relaxation time of the Hydrogen atoms that form the main part of the fat and water molecules of the body and hence improve the MR image contrast, especially in regions containing high fraction of these materials [6]. Among the above-mentioned oxides, Fe_3O_4 nanoparticles have been widely investigated due to their good biocompatibility. For this purpose, various surfactant stabilizers such as Dextran, PVP, PVA and PEG have been used to synthesize stable suspensions of magnetite nanoparticles with desired particle size distribution. According to the literature, particles with a size between 80 and 150 nanometers mainly accumulate in the liver and spleen [7]. These values are related to the hydrodynamic size of particles including the magnetite aggregates and the absorbed surfactant shell, not only the magnetite core. To this value, the size of the surface-absorbed molecule layer of the liquid phase is added. This recent value is more in the case of hydrophilic surfactants such as dextran in aqueous media. It has also been previously shown that particle hydrodynamic size is strongly affected by the sample concentration [8]. In order

* *Corresponding Author Email: re.ahmadi@eng.ikiu.ac.ir*

to determine the target tissue, hydrodynamic size is to be measured in the concentration of sample in the body. Sample concentration decreases after injection into blood, so this concentration must be considered instead of the original concentration before administration.

Among conventional methods of synthesizing magnetite nanoprticles including thermal decomposition [9], hydrothermal processes [10, 11], co-precipitation [8, 12] and sol-gel [13], thermal ones such as the hydrothermal method lead to formation of monodisperse particles with a narrow size distribution histogram. In addition, these approaches are more controllable and repeatable with a high yield of magnetite nanoparticles. Despite these advantages, they are not applicable for biological aims immediately after synthesis. Since thermal synthesis approaches lead to formation of fatty acid capped particles (for example oleic acid capped particles), they are not dispersible in aqueous solutions suitable for biological applications and a supplementary surface exchange step is essential to make them suitable for water-based ferrofluids [14]. Moreover, these approaches usually are performable at high temperatures exceeding 200°C and the as-synthesized products are not biocompatible [15].

In this work, a low temperature hydrothermal process is employed for synthesizing oleic acid capped magnetite nanoparticles. This approach has been introduced by this group previously [16]. Instead of transferring obtained particles into water for injecting into animals, they have been directly dispersed in Ethiodol which is a biocompatible poppy seed oil. This oil has not been used for synthesizing MRI contrast agents before, but has been employed for other biological applications [17]. By using this approach, there is no need for any supplementary surface exchange stage for dispersing particles in water. The obtained Ethiodol based ferrofluid was directly injected into rats to investigate possibility of its use as a potential MRI contrast agent. Furthermore, as pure Ethiodol is known as a CT imaging contrast agent, the obtained Ethiodol based contrast agent can be considered as a dual imaging MRI-CT contrast agent. This is the topic of our undergoing investigations.

MATERIALS AND METHODS

Oleic acid, DMSO, $FeCl_2.4H_2O$ and TMAH all were prepared with analytical grade from Sinopharm Chemical Reagent Co. Oleic acid capped magnetite nanoparticles were synthesized via a low temperature one step process accordingly: $FeCl_2.4H_2O$ and oleic acid were dissolved in DMSO to make a solution with the molarities of 0.1 and 0.8 for $FeCl_2$ and oleic acid respectively. This solution was magnetically stirred for 10 minutes under an N_2 atmosphere. After that, the temperature was raised to 140°C and 15 mmole TMAH 25% v/v was added into the reaction container under an N_2 atmosphere while magnetic stirring was in progress. The reaction was in run for 60 minutes and a black product gradually formed. This product was extracted from the liquid phase using magnetic separation and was washed 3 times with acetone. One part of this solid was used for XRD and VSM characterizations after vacuum drying and the remainder was dispersed in n-hexane for TEM and AFM studies (Sample A). The abovementioned synthesis process was repeated in the presence of 10 mmole TMAH 25% v/v instead of 15 mmole to investigate effect of solution alkalinity on particle size distribution (Sample B).

Evaluation of Cellular Uptakes

Qualitative evaluation of magnetic nanoparticle internalization was done by Prussian blue patch. Iron deposition within the cells was monitored by characteristic blue color of Prussian blue. For this study, HeLa cells were obtained from Pasteur institute National Cell Bank of Iran (NCBI) and grown on DMEM F12 medium for 48 h after which they were exposed to 60µg(Fe)/ml sample A for 4 h. After washing with PBS, cells were immersed in a mixture containing equal volumes of 20% aqueous solution of HCl and 10% aqueous solution of potassium ferrocyanide [$K_4Fe(CN)_6.\ 3H_2O$] for 20 minutes. The quantitative determination of intracellular iron uptake was done by inductively coupled plasma spectroscopy (ICP). For this step, the cells were incubated in magnetic nanoparticle and then washed 3–4 times thoroughly with phosphate buffer saline solution (pH 7.4) and trypsinized. Cells were then centrifuged at 1000g for 10 min to form a pellet of cells. The cell pellet was dissolved in nitric acid to digest the cells and release ferric iron ions from ferrite particles. Finally concentration of Fe ions in the solution was measured by ICP-AES. It is noteworthy that the number of cells were counted using a hemocytometer.

MTT-Tetrazolium Assay

The safety of nanoparticles on HeLa cancer cells was tested using the MTT assay method [18], which measures the ability of metabolically active mitochondria in live cells to reduce a yellow tetrazolium compound to a purple formazan product. The HeLa cancer cells (10^6 cells/ml) were treated with different concentrations of sample A nanoparticles (30, 60 and 120 µg(Fe)/ml) then the media was removed, and 100 µl of culture media without FCS and 10 µl of MTT (5 mg/ml in PBS) were added to each well and cells were incubated. After 4 h, the media was removed from the wells, and the cells were lysed with 200 µl of DMSO. After the formazan product was dissolved, the absorbance at 545 nm was measured using an ELISA reader (Stat Fax-2100 Awareness, Mountain View, CA, USA). Eight replicates were used for each situation, and the experiments were repeated three times. Relative survival was represented as the absorbance of the treated sample/absorbance of the control group.

MRI Study

For MRI studies, 0.1 gram of the product was dispersed in Ethiodol via ultrasonic irradiation to make a 2 mg (Fe)/ml solution. This suspension was used as the potential MRI contrast agent.

Characterization

XRD patterns were taken by a Siemens D5000 X-ray theta/theta diffractometer using graphite monochromatized high intensity CuK_{α} radiation (λ=1.5406 °A) via movement of both the X-ray source and detector. A JEOL TEM JEM2010F was used to determine the average particle size and morphology of the powders on an accelerating voltage of 200 kV. A Beckman-Coulter N4-plus submicron particle size analyzer was employed for hydrodynamic diameter measurement via PCS technique. Magnetometry was carried out on solid samples at 300 K with a Lakeshore 7470 VSM instrument over a range of applied fields between -10000 and +10000 Oersted.

RESULTS AND DISCUSSION

TEM

TEM images of samples A and B synthesized in the presence of 15 and 10 mmole TMAH are shown in Fig. 1 with mean particle sizes of 4.5 and 9.6 nm, respectively. Particles are semispherical in shape with rather narrow size distribution diagrams. The effect of TMAH amount on particle size can be explained as follows: decrease of TMAH leads to decrease of OH^- on particle surfaces and increase of particle growth rate due to decrease of electrostatic repulsion forces between the initial magnetite nucleuses. Hence, particle size increases with the decrease in the amount of TMAH.

AFM

When one drop of ferrofluid is put on the silicon surface for AFM study, it will dry after several minutes and some agglomerates containing magnetite particles may form due to surface tension effects. Therefore, the height and width of the agglomerates determined by AFM image can show the size of individual particles and formed agglomerates, respectively.

An AFM image of sample A is shown in Fig. 2. As shown in this image, the scanned height (thickness) and width (diameter) of the agglomerate can be determined from AFM images. Five agglomerates are marked in Fig. 2. The width of agglomerates

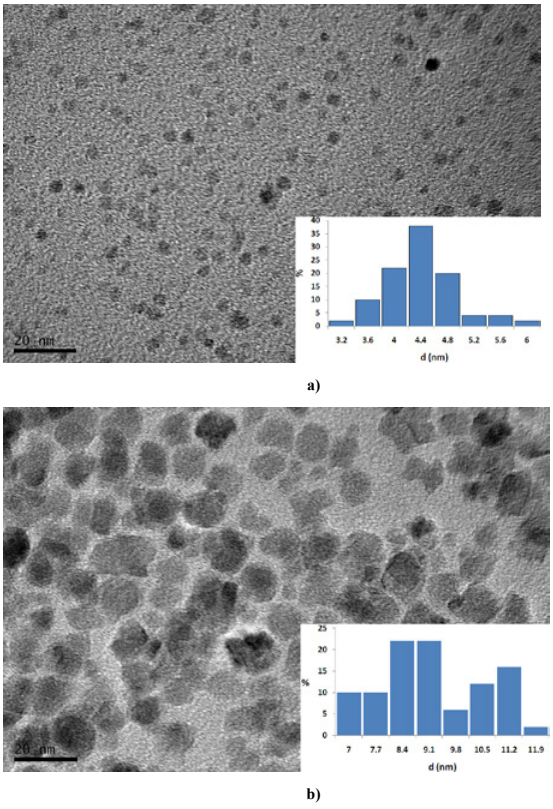

Fig. 1. TEM image of samples synthesized in the presence of a) 10 mmole TMAH (sample A) and b) 15 mmole TMAH (sample B).

can be found from the vertical red lines. These sizes are determined as 73.3, 61.0, 113.3, 80.5 and 75.2 nm for agglomerates 1 to 5, respectively. The horizontal green lines related to agglomerate 4 are presented in Fig. 2 as well. Particle size can be determined as 75 A° from this image. These sizes are comparable with the TEM image of sample A, including particles in the range of 7 to 12 nanometers (Fig. 1-a).

XRD

The XRD patterns of samples A and B are presented in Fig. 3. Six characteristic peaks including (200), (311), (400), (422), (511) and (440) are identified in bragg angles 30.15, 35.56, 43.06, 53.20, 57.04 and 62.63°. These are characteristic peaks of the pure magnetite (JPDCS card no. 9-0629). Using the Scherrer equation, the particle size is calculated as 5.2 and 10.5 nm for samples A and B, respectively, which are close to TEM results.

VSM

VSM diagrams of samples A and B with saturation magnetizations of 42.5 and 64.7 emu/g are shown in Fig. 4. Superparamagnetic behavior of these samples is related to their small size so their heat energy (kT) is much larger than their magnetic anisotropic energy (KV) where k is the Boltzmann constant, T is the absolute temperature, K is the magnetic anisotropy constant of magnetite nanoparticles and V is the nanoparticle volume. In these conditions, no permanent magnetic moment and magnetic ordering form due to large thermal vibrations. The high value of the saturation magnetization of the samples (especially sample B with a larger mean particle size) as opposed to conventional magnetite nanoparticles used as MRI contrast agents is mainly due to the presence of the low molecular weight oleic acid as the surfactant (M_w= 282.46 g/mol) instead of the conventional high molecular weight surfactants such as dextran and

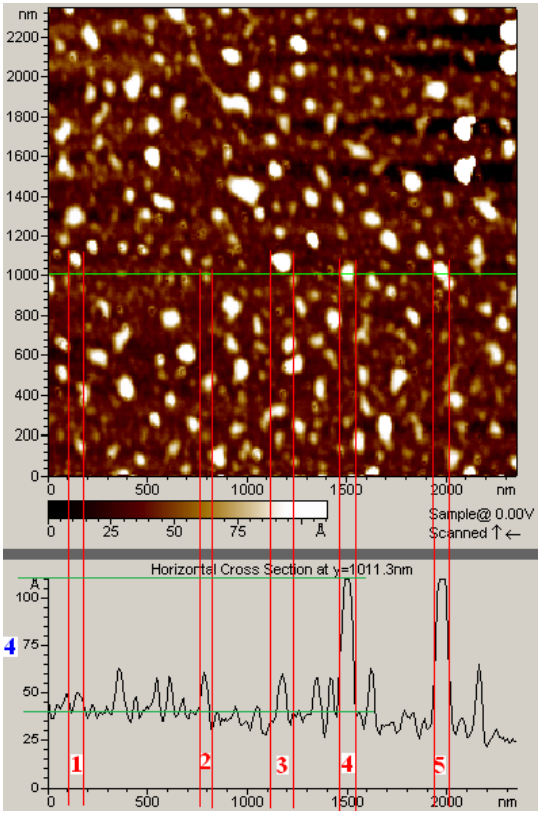

Fig. 2. AFM image of sample A

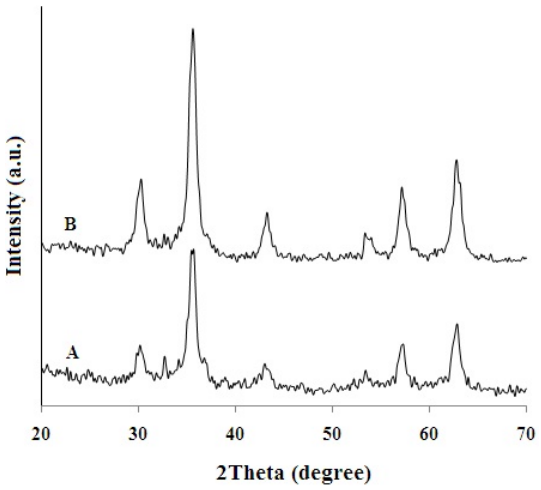

Fig. 3. XRD patterns of samples A and B

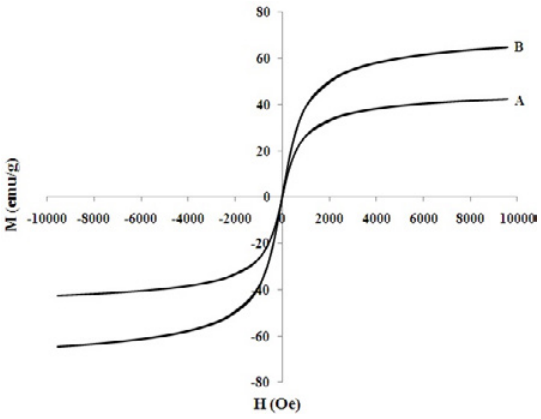

Fig. 4. VSM diagrams of samples A and B revealing their superparamagnetic behavior.

PEG. Therefore, the fraction of the non-magnetic phase decreases and saturation magnetization increases. This large saturation magnetization leads to MR images with better contrast and higher quality due to more effective shortening of T2 relaxation time in the region of nanoparticle accumulation [1].

In Vitro Cell Labeling

After 4 h of cell incubation in SPIO nanoparticles sample A, more than 90% of the HeLa cells displayed positive results upon Prussian blue staining. Prussian blue patch monitored iron-containing sites as blue spots in the cytoplasm (Fig. 5). In addition, Fe/ml concentration for 200 hundred cells, measured by ICP, was 0.26 ppm.

Cell Viability Assay

The effect of different concentrations of nanoparticles in sample A on the viability of HeLa cells is depicted in Fig. 6. In these concentrations, synthesized nanoparticles did not induce complete cell death in HeLa cells. The maximum reduction in cell survival was observed when cells were treated with sample A with a concentration of 120 µg(Fe)/ml. The cell viability was 92% at this concentration so the particles viability is suitable.

MRI results

In order to obtain stable ferrofluid of magnetite nanoparticles in Ethiodol, 50 mg of the dried sample A was dispersed in Ethiodol via 60 minutes ultrasonic irradiation at 40kHz and 30°C. The

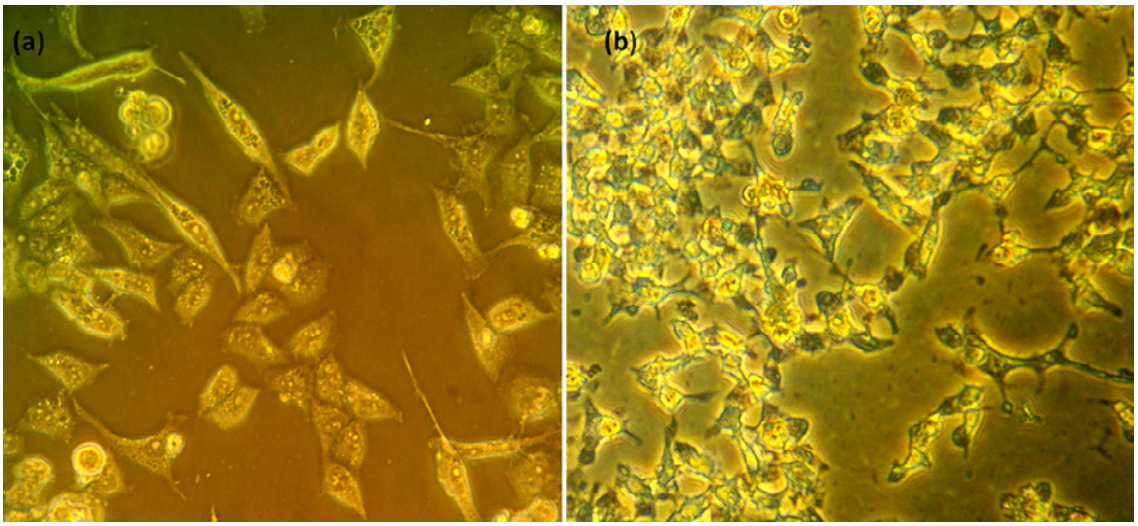

Fig. 5. Follow-up of nanoparticles uptake with Prussian blue staining after 4 h incubation for (a) negative control (complete culture medium) and (b) sample A 60 µg(Fe)/ml.

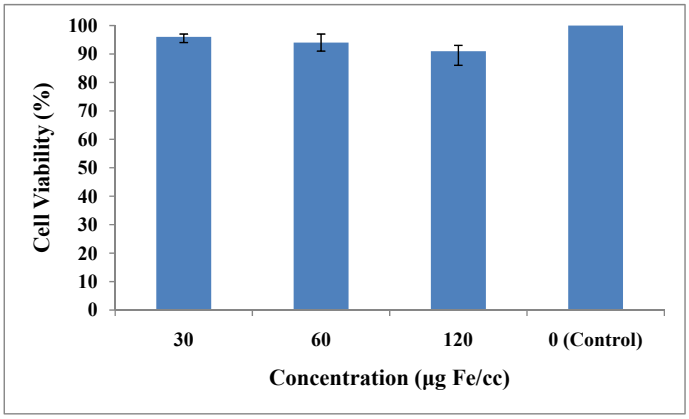

Fig. 6. Viability of Hela cells after 4 h incubation with sample A, verifying the acceptable biocompatibility of over 91% in all concentrations.

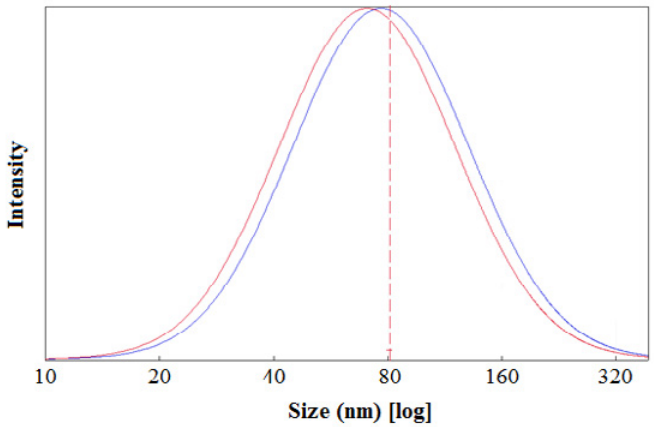

Fig. 7. PCS histogram of sample A1.

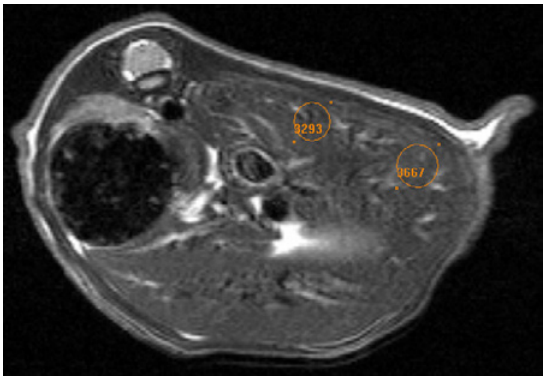

a)

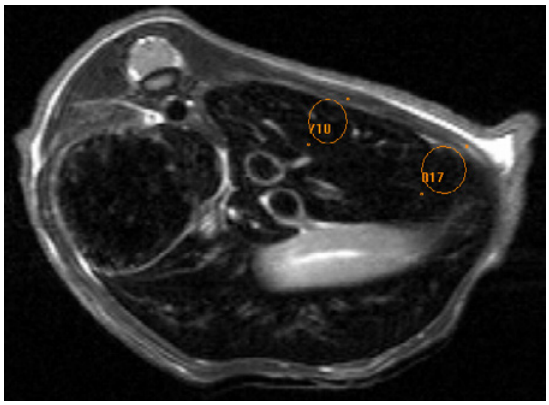

b)

Fig. 8. MR image of a mouse a) before injection and b) 30 minutes after IV injection of sample A1. Signal intensity decrease is evident in the elliptical shown regions of liver.

concentration of the obtained ferrofluid was 0.2 mg (Fe)/cc (Ferrofluid A1). Hydrodynamic size histogram of this ferrofluid is shown in Fig. 7 with mean hydrodynamic size of 81.1nm. This histogram was obtained using PCS measurements and repeated 2 times. The stable ferrofluid has been intravenously injected into 20 g mice via lateral tail vein at a dose of 2 mg (Fe)/kg body weight. The MR images of the mouse before and 30 minutes after IV injection are presented in Figs. 8-a and 8-b. As clearly seen in these images, the liver becomes darker after injection and the respective signal intensity decreases from 3667 and 3293 to 817 and 710 in the elliptical shown regions. This is a sign of magnetite particle accumulation in liver. According to the theory, particles with a mean hydrodynamic size between 80 and 150 nm mainly accumulate in liver and spleen and increase image contrast through a remarkable shortening of T_2 relaxation time [19]. This is coincides positively with the results shown in Fig. 8-b. According to these MR images, the synthesized Ethiodol-based ferrofluid is a suitable potential MRI contrast agent.

CONCLUSION

In this work, monodisperse oleic acid capped magnetite nanoparticles with mean particle sizes of 4.5 and 9.6 nanometers were successfully synthesized via a low temperature hydrothermal process. XRD results verified the reverse spinel structure of the product to be similar to pure magnetite. VSM results show the superparamagnetic behavior of samples with saturation magnetizations of 42.6 and 64.7 emu/g. Due to the usage of the single molecule acid oleic surfactant instead of conventional polymeric ones such as Dextran and PEG, the saturation magnetization increased significantly in contrast to conventional MRI agents. According to the MTT assay results, the obtained particles were

biocompatible. Hydrodynamic size distribution diagram of the Ethiodol suspension containing the synthesized particles verified its suitability for imaging and drug delivery into liver and spleen. This corresponded positively with MRI results showing particle accumulation in these organs. Thus, a new oil base MRI contrast agent is introduced in this work, especially for liver and spleen imaging.

CONFLICT OF INTERESTS

The authors declare that there is no conflict of interests regarding the publication of this paper.

REFERENCES

1. Li J, Wang S, Wu C, Dai Y, Hou P, Han C, et al. Activatable molecular MRI nanoprobe for tumor cell imaging based on gadolinium oxide and iron oxide nanoparticle. Biosensors and Bioelectronics. 2016;86:1047-53.
2. Ahmadi R, Hosseini M, Masoudi A. Avrami behavior of magnetite nanoparticles formation in co-precipitation process. Journal of Mining and Metallurgy, Section B: Metallurgy. 2011;47(2):211-8.
3. Omid H, Oghabian MA, Ahmadi R, Shahbazi N, Hosseini HRM, Shanehsazzadeh S, et al. Synthesizing and staining manganese oxide nanoparticles for cytotoxicity and cellular uptake investigation. Biochimica et Biophysica Acta (BBA) - General Subjects. 2014;1840(1):428-33.
4. Ahab A, Rohman F, Iskandar F, Haryanto F, Arif I. A simple straightforward thermal decomposition synthesis of PEG-covered Gd 2 O 3 (Gd 2 O 3 @PEG) nanoparticles. Advanced Powder Technology. 2016;27(4):1800-5.
5. Babić-Stojić B, Jokanović V, Milivojević D, Požek M, Jagličić Z, Makovec D, et al. Gd2O3 nanoparticles stabilized by hydrothermally modified dextrose for positive contrast magnetic resonance imaging. Journal of Magnetism and Magnetic Materials. 2016;403:118-26.
6. Hendrick RE, Mark Haacke E. Basic physics of MR contrast agents and maximization of image contrast. Journal of Magnetic Resonance Imaging. 1993;3(1):137-48.
7. LaConte L, Nitin N, Bao G. Magnetic nanoparticle probes. Materials Today. 2005;8(5):32-8.
8. Ahmadi R, Hosseini HRM, Masoudi A, Omid H, Namivandi-Zangeneh R, Ahmadi M, et al. Effect of concentration on hydrodynamic size of magnetite-based ferrofluid as a potential MRI contrast agent. Colloids and Surfaces A: Physicochemical and Engineering Aspects. 2013;424:113-7.
9. Glasgow W, Fellows B, Qi B, Darroudi T, Kitchens C, Ye L, et al. Continuous synthesis of iron oxide (Fe3O4) nanoparticles via thermal decomposition. Particuology. 2016;26:47-53.
10. Cannio M, Ponzoni C, Gualtieri ML, Lugli E, Leonelli C, Romagnoli M. Stabilization and thermal conductivity of aqueous magnetite nanofluid from continuous flows hydrothermal microwave synthesis. Materials Letters. 2016;173:195-8.
11. Attallah OA, Girgis E, Abdel-Mottaleb MMSA. Synthesis of non-aggregated nicotinic acid coated magnetite nanorods via hydrothermal technique. Journal of Magnetism and Magnetic Materials. 2016;399:58-63.
12. Macías-Martínez BI, Cortés-Hernández DA, Zugasti-Cruz A, Cruz-Ortíz BR, Múzquiz-Ramos EM. Heating ability and hemolysis test of magnetite nanoparticles obtained by a simple co-precipitation method. Journal of Applied Research and Technology. 2016;14(4):239-44.
13. Sciancalepore C, Bondioli F, Manfredini T, Gualtieri A. Quantitative phase analysis and microstructure characterization of magnetite nanocrystals obtained by microwave assisted non-hydrolytic sol–gel synthesis. Materials Characterization. 2015;100:88-97.
14. Wu, Y., Wang, C., Wu, L., Yang, T., Zhang, X. and Zhang, Y., Ultrasmall superparamagnetic particles of iron oxide modified with small molecules of DMSA. In: The Seventh China-Korea Symposium on Biomaterials and Nano-Biotechnology, China; 2009.
15. Wang J, Sun J, Sun Q, Chen Q. One-step hydrothermal process to prepare highly crystalline Fe3O4 nanoparticles with improved magnetic properties. Materials Research Bulletin. 2003;38(7):1113-8.
16. Ahmadi R, Masoudi A, Madaah Hosseini HR, Gu N. Kinetics of magnetite nanoparticles formation in a one step low temperature hydrothermal process. Ceramics International. 2013;39(5):4999-5005.
17. Ruizhi X, Hui Y, Yu Z, Ming M, Zhongping C, Changling W, et al. Three-Dimensional Model for Determining Inhomogeneous Thermal Dosage in a Liver Tumor During Arterial Embolization Hyperthermia Incorporating Magnetic Nanoparticles. IEEE Transactions on Magnetics. 2009;45(8):3085-91.
18. Montazerabadi A-R, Sazgarnia A, Bahreyni-Toosi MH, Ahmadi A, Shakeri-Zadeh A, Aledavood A. Mitoxantrone as a prospective photosensitizer for photodynamic therapy of breast cancer. Photodiagnosis and Photodynamic Therapy. 2012;9(1):46-51.
19. Kalber TL, Smith CJ, Howe FA, Griffiths JR, Ryan AJ, Waterton JC, et al. A Longitudinal Study of R2* and R2 Magnetic Resonance Imaging Relaxation Rate Measurements in Murine Liver After a Single Administration of 3 Different Iron Oxide-Based Contrast Agents. Investigative Radiology. 2005;40(12):784-91.